Journal of Neuroendocrinology

Journal of Neuroendocrinology, 2013, **25**, 1241–1254

ORIGINAL ARTICLE

Annexin A1 Complex Mediates Oxytocin Vesicle Transport

V. Makani*, R. Sultana†, K. S. Sie*, D. Orjiako*, M. Tatangelo*, A. Dowling‡, J. Cai§, W. Pierce§, D. Allan Butterfield†, J. Hill‡ and J. Park*

**Department of Neurosciences, College of Medicine, University of Toledo, Toledo, OH, USA.*

†*Department of Chemistry, University of Kentucky, Lexington, KY, USA.*

‡*Department of Physiology and Pharmacology, College of Medicine, University of Toledo, Toledo, OH, USA.*

§*Department of Pharmacology and Toxicology, University of Louisville, Louisville, KY, USA.*

Journal of Neuroendocrinology

Oxytocin is a major neuropeptide that modulates the brain functions involved in social behaviour and interaction. Despite of the importance of oxytocin for the neural control of social behaviour, little is known about the molecular mechanism(s) by which oxytocin secretion in the brain is regulated. Pro-oxytocin is synthesised in the cell bodies of hypothalamic neurones in the supraoptic and paraventricular nuclei and processed to a 9-amino-acid mature form during post-Golgi transport to the secretion sites at the axon terminals and somatodendritic regions. Oxytocin secreted from the somatodendritic regions diffuses throughout the hypothalamus and its neighbouring brain regions. Some oxytocin-positive axons innervate and secrete oxytocin to the brain regions distal to the hypothalamus. Brain oxytocin binds to its receptors in the brain regions involved in social behaviour. Oxytocin is also secreted from the axon terminal at the posterior pituitary gland into the blood circulation. We have discovered a new molecular complex consisting of annexin A1 (ANXA1), A-kinase anchor protein 150 (AKAP150) and microtubule motor that controls the distribution of oxytocin vesicles between the axon and the cell body in a protein kinase A (PKA)- and protein kinase C (PKC)-sensitive manner. ANXA1 showed significant co-localisation with oxytocin vesicles. Activation of PKA enhanced the association of kinesin-2 with ANXA1, thus increasing the axon-localisation of oxytocin vesicles. Conversely, activation of PKC decreased the binding of kinesin-2 to ANXA1, thus attenuating the axon-localisation of oxytocin vesicles. The result of the present study suggest that ANXA1 complex coordinates the actions of PKA and PKC to control the distribution of oxytocin vesicles between the axon and the cell body.

Key words: oxytocin, annexin A1, kinesin-2, AKAP150, protein kinase A, protein kinase C

doi: 10.1111/jne.12112

Correspondence to:
Joshua Park, Department of Neurosciences, College of Medicine, University of Toledo, Toledo, OH 43614, USA (e-mail: joshua.park2@utoledo.edu).

Pro-oxytocin is synthesised in the cell bodies of hypothalamic neurones in the supraoptic (SON) and paraventricular (PVN) nuclei of the hypothalamus and is processed to a 9-amino-acid mature form during post-Golgi transport to the secretion sites at the axon terminals and somatodendritic regions (1,2). The axon terminals of PVN neurones innervate the posterior pituitary gland (neurohypophysis) and secrete oxytocin directly into the bloodstream. Plasma oxytocin facilitates lactation, parturition and natriuresis, and also reduces blood pressure and heart rate (3–6). Oxytocin secreted from the soma and dendrites diffuses throughout the hypothalamus and the neighbouring brain regions of the hypothalamus. Oxytocin-positive axons also innervate and secrete oxytocin into the amygdala, septum, substantia nigra, stria terminalis, olfactory bulb, brainstem (nucleus tractus solitarius) and spinal cord (7–14). Oxytocin secreted inside the brain affects brain functions involved in behaviour, anxiety, cognition and autonomic nerve activity (15).

Acute oxytocin secretion at the axon terminal differs from that at the somatodendritic region with respect to its sensitivity to membrane depolarisation and calcium. Plasma membrane depolarisation by high K^+ induces axonal (but not somatodendritic) oxytocin secretion (16). Conversely, somatodendritic (but not axonal) oxytocin secretion is induced by increased cytoplasmic calcium ($[Ca^{2+}]_i$) (16,17). In addition to the differential sensitivity to membrane depolarisation and Ca^{2+} influx, axonal and somatodendritic oxytocin secretion appears to be affected differently by protein kinase A (PKA) and protein kinase C (PKC). Activation of the seroto-

ninergic receptors increases cAMP, a PKA activator, and enhances axonal oxytocin secretion to the neurohypophysis (18,19). Glucagon-like peptide-1 is released from the neurones of the nucleus of the solitary tract that innervate into the PVN and causes accumulation of oxytocin vesicles at the axon terminal in the pituitary gland in a PKA-dependent manner (20). Norepinephrine and prolactin releasing peptide released from neurones of the medulla oblongata innervating into the PVN also increase axonal oxytocin secretion from the neurohypophysis (21).

Conversely, signalling pathways that increase $[Ca^{2+}]_i$ and activate PKC facilitate somatodendritic oxytocin secretion. α-Melanocyte stimulating hormone (MSH) that increases $[Ca^{2+}]_i$ and activates PKC via the G_q receptor enhances somatodendritic oxytocin secretion (16). Simultaneously, α-MSH decreases axonal oxytocin secretion by reducing cAMP via the $G_{i/o}$ receptor and attenuating the membrane potential of oxytocin neurones (16). Endocannabinoids have a similar effect on the secretion of oxytocin (22). Galanin, an activator of the $G_{i/o}$ receptor, appears to decrease axonal oxytocin secretion by inhibiting PKA (23).

All of these previous studies demonstrate the effects of extracellular stimuli on the exocytosis of oxytocin vesicles from secretion sites at the axon terminals and somatodendritic regions. However, little is known about the molecular mechanism by which the distribution of oxytocin vesicles between the axon and the somatodendritic region is regulated by extracellular stimuli. We have discovered a molecular complex consisting of annexin A1 (ANXA1), A-kinase-associated protein 150 (AKAP150) and kinesin-2 that coordinates the actions of PKA and PKC to enhance and attenuate, respectively, the targeting of oxytocin vesicles to the axon terminals.

A-kinase anchor protein 5 (AKAP5 = rat AKAP150 = human AKAP79) binds to PKA and PKC and coordinates their phosphorylation actions (24–28). AKAP5 targets the phosphorylating action of PKA to AMPA receptor (29,30). AKAP5 also coordinates PKC-mediated phosphorylation of voltage-gated M-type K^+ channels (31,32). By contrast, little is known about the function of AKAP5 in hormone secretion. AKAP5 coordinates glucagon-like peptide-1-induced enhancement of insulin secretion (33,34). In melanocytes, AKAP5 appears to form a complex with PKA, kinesin-2, cytoplasmic dynein and dynactin on melanosomes, thus affecting the direction of melanosome transport (35).

ANXA1, a phospholipid/Ca^{2+}-binding protein (36), is abundant in the pituitary gland and, to lesser extent, in the hypothalamus (37). ANXA1 mediates some of the steroid-mediated stress responses (38,39). Glucocorticoids increase the *de novo* synthesis of ANXA1 (40) and cause the extracellular secretion of ANXA1 (41). In pancreatic β cells, ANXA1 was almost exclusively observed on most of the insulin-containing vesicles (approximately 90%) (42), suggesting that ANXA1 may mediate the interaction of vesicles with cytoplasmic machinery. According to a recent finding in which knockout of ANXA1 blocked the anterograde transport of Shiga toxin (43), one of the AXNA1-interacting cytoplasmic machineries appears to be microtubule-based transport system Hence, ANXA1 may be involved in intracellular trafficking of hormone-containing vesicles.

In the present study, we demonstrate how ANXA1 mediates the anterograde transport of oxytocin vesicles via its interaction with kinesin-2 and AKAP150 in PKA- and PKC-sensitive manners.

Materials and methods

Antibodies and materials

The 4659 and 4660 antibodies were gifts from Dr Y. Peng Loh (NIH, Bethesda, MD, USA). The 4659 and 4660 antibodies were generated against the recombinant protein of full-length snapin in chicken by AVES Labs, Inc. (Tigard, OR, USA). In accordance with the manufacturer's protocol, antigen was injected four times into the breast muscle of chicken: the first in complete Freunds' adjuvant and the remaining injections at a 1 : 1 dilution of complete and incomplete Freunds' Adjuvants. One week after the fourth injection, the immunoglobulin (Ig)Y batches (4659 and 4660) were purified from pre-immune and immune eggs. Anti-snapin antibody (clone L8/15) was purchased from NeuroMab Inc. (Davis, CA, USA). Antibodies to ANXA1 (sc-12740), AKAP150 (sc-10765), dynein intermediate chain (DIC, sc-13524), kinesin-1 (kinesin heavy chain, sc-28538), kinesin-2 (KIF3A, sc-135960), carboxypeptidase E (CPE) (sc-136252), dynactin (p150, sc-11363) and syntaxin-1 (sc-12736) were purchased from Santa Cruz Biotechnology (Santa Cruz, CA, USA). Antibodies to microtubule-associated protein 2 (MAP2) (610460), kinesin-2 (KIF3A, 611508), kinesin-3 (KIF1A, 612094), p115 (612260), CPE (610758) and calreticulin (612137) were obtained from BD Biosciences (San Jose, CA, USA). Anti-synaptophysin antibody (S5768) was obtained from Sigma (St Louis, MO, USA). Anti-oxytocin antibody (ab2078) was obtained from Abcam (Cambridge, MA, USA). Forskolin, PKI-ester and phorbol ester [phorbol 12-myristate 13-acetate (PMA)] were purchased from Sigma and dissolved in dimethyl sulphoxide (DMSO) (Sigma). Control and annexin-1 short hairpin (sh)RNA lentiviral particles and Polybrene® were purchased from Santa Cruz Biotechnology.

GST-ANXA1 expression and purification

Glutathione-*S*-transferase (GST) tagged ANXA1 was generated by inserting the *Bam*HI-*Xho*I digest of the polymerase chain reaction product of annexin-1 cDNA in GFP-ANXA1 that was purchased from Origene Co. (Rockville, MD, USA) into pGEX4T-2. GST tag alone or GST-tagged ANXA1 was purified on 40 μl of glutathione (GSH) beads (Novagen Co., Madison, WI, USA) from bacterial cell cytosol in 5 ml of Bugbuster solution (EMD Chemicals Inc., San Diego, CA, USA) containing protein inhibitor cocktails. After extensive washing in phophate-buffered saline (PBS), GST proteins were eluated from GSH beads in 100 μl of 10 mM GSH + protein inhibitor cocktails. The eluate from the GSH beads was mixed with 40 μl sodium dodecylsulphate (SDS) loading buffer and loaded onto NuPAGE SDS gel (Invitrogen, Carlsbad, CA, USA) for immunoblotting.

Cell culture and drug treatment

AtT20 cells that were used for our study are F2 subclone [AtT-20/D16V-F2, ATCC® CRL-1795TM, ATCC (Manassas, VA, USA)]. The F2 subclone of AtT20 cells is different from the D1 and D16 subclones of AtT20 cells that do not express endogenous ANXA1 (44). N11 cells were purchased from Cedarlane Co. (Burlington, NC, USA). N11 cells are cloned from mouse embryonic hypothalamic primary cultures immortalised by retroviral transfer of SV40 T-Ag. N11 cells express oxytocin, steroidogenic factor 1 (SF-1) and other hypothalamic neurone markers. Both AtT20 (passages 14–16) and N11 cells (passages 2–3) were grown in Dulbecco's modified Eagle's medium [DMEM (Life Technologies, Grand Island, NY, USA)] containing 10% heat-inactivated fetal bovine serum, 1 g/l D-glucose, 110 mg/l sodium pyruvate, and 1× Pen Strap (Life Technologies). To obtain primary hypothalamic neurones, female preg-

nant mice (BALB/C; Charles River Laboratories International, Inc., Wilmington, MA, USA) at gestation day 17 (E17) were anaesthetised and dissected to obtain eight or nine embryos per mouse. Cortical neurones were isolated from embryonic brains and differentiated on poly-L-lysine-coated coverslips in B27/neurobasal medium for 14 days (DIV14). All the cell cultures were incubated at 37 °C in a humidified 5% CO_2 incubator. For drug treatment, N11 cells or primary hypothalamic neurones were treated with DMSO (0.1%), 10 μM forskolin or 10 nM PMA before immunocytochemistry and immunoprecipitation.

Transduction

Transduction of shRNA lentiviral particles (sc-29198-V; Santa Cruz Biotechnology) was conducted in accordance with the manufacturer's instructions. The shRNA lentiviral particles contain four expression constructs each encoding target-specific 19–25 nucleotides (plus hairpin) shRNA designed to knockdown ANXA1. Primary hypothalamic neurones (E17, DIV14) differentiated on coverslips in 24-well plates were incubated in 0.5 ml of B27/neurobasal medium containing 5 μg/ml Polybrene® and 3 μl of shRNA particles (15 000 infectious units of virus) for 24 h. On the second day of transduction, the medium containing shRNA particles was replaced with fresh medium minus shRNA particles and incubated for 5 days before immunocytochemistry.

Immunocytochemistry

For microscopic purposes, neurones or N11 cells cultured on poly-L-lysine-coated coverslips were fixed at 37 °C in DMEM medium containing 3.7% paraformaldehyde for 30 min, and permeabilised with 0.1% Triton X-100 in PBS for 30 min. After blocking with 2% bovine serum albumin (BSA) in T-TBS (Tris-buffered saline+ 0.1% Tween 20), neurones or cells were immunostained with primary antibodies. Bound primary antibodies were detected using their corresponding secondary antibodies conjugated with $Alexa_{488\ nm}$ or $Alexa_{594\ nm}$ (Life Technologies). Coverslips were then mounted on glass slides using Fluoromount G (Fisher Scientific Co., Pittsburgh, PA, USA).

Confocal microscopy and image analysis

The images of immunostained neurones and N11 cells were taken using a TCS SP5 multi-photon laser scanning confocal microscope (Leica Microsystems, Bannockburn, IL, USA). The confocal microscope is equipped with conventional solid state, a ti-sapphire tunable multi-photon laser (Coherent, Santa Clara, CA, USA) and an acousto optical beam splitter. Images were taken with a × 63 Zeiss alpha plan fluor oil objective (1.4 NA). METAMORPH software (Life Technologies) was used to quantify the intensity of oxytocin and ANXA1 in the axons, axon terminals and the cell body. The correlation co-efficient of co-localisation (CCC) between ANXA1 and oxytocin vesicles was obtained using METAMORPH as described by Park *et al.* (45). The region of interest was limited to either the whole cell or a small cell region per image. According to the developer of METAMORPH, $CCC = \sum_i[S_c1_i \times S_c2_i]/SQRT(\sum_i[S1_i]^2 \times \sum_i[S2_i]^2)$, where i is the i_{th} pixel in the region of interest, S_c1 is the signal intensity of pixel involved in co-localisation in the first channel, S_c2 is the signal intensity of pixel involved in co-localisation in the second channel, $S1$ is the signal intensity of pixel, regardless of co-localisation, in the first channel, $S1$ is the signal intensity of pixel, regardless of co-localisation, in the second channel and *SQRT* is the square root. To obtain data objectively, all of the image were acquired and analysed blindly by different persons.

In-gel trypsin digestion and mass spectrometry

A protein band of 38 kDa was excised from coomassie-stained NuPAGE gel with a clean, sterilised blade and transferred to Eppendorf microcentrifuge tubes. In-gel trypsin digestion and mass spectrometry were conducted as described previously (46).

Co-immunoprecipitation

For coimmunoprecipitation studies, the cytosols of N11 cells or mouse hypothalamus tissues were prepared. N11 cells from eight 100-mm dishes at approximately 90% confluency or three hypothalami (BALB/C, female, 8-weeks) were harvested and resuspended in 1.2 ml of PMEE buffer (pH 7.0; 35 mM KOH, 35 mM PIPES, 5 mM $MgSO_4$, 1 mM ethylene glycol tetraacetic acid, 1% BSA and 0.5 mM ethylenediaminetetraacetic acid) containing 1 mM 4-(2-aminoethyl) benzenesulfonyl fluoride hydrochloride and 1× Halt™ protease inhibitor cocktail (Thermo Scientific, Rockford, IL, USA). Cells were then ruptured by passing them through a 27-gauge needle (Becton Dickinson, Franklin Lakes, NJ, USA) 20 times to break down any vesicular structures. Cell debris and nuclear membranes were removed by centrifugation for 20 min at 14 500 **g** to obtain post-nuclear supernatant. Then, 1 ml of the post-nuclear supernatant (5 mg/ml protein) was split into two sets of 500 μl. Each 500 μl of the cytosol was mixed with 100 μl of protein A-agarose beads (Sigma) and incubated for 1 h at 4 °C on a rotating platform to preclear the cytosol. After removal of the agarose beads, the cytosol was mixed with either 5 μg of control IgGs or IgGs against ANXA1 or p150 (dynactin) and incubated for 16 h at 4 °C. Then, 60 μl of protein A-agarose beads was added to the tubes and incubated for 8 h. After incubation, the beads were washed four times with PMEE buffer and boiled in 60 μl of SDS loading buffer. Co-immunoprecipitation was performed twice per condition.

Differential centrifugation

N11 cells were harvested from three 100-mm culture dishes of approximately 90% confluency. Hypothalamic tissues were dissected from two mice (BALB/C, female, 8- weeks) and used for differential centrifugation. After washing with PBS, cell pellet or hypothalamic tissue was resuspended in 0.3 ml of PMEE buffer + proteases/phosphatases inhibitors + 0.25 M sucrose (PMEE-IS) and passed through a 27-gauge needle six times. A post-nuclear supernatant (0.5–1 mg/ml) was generated from the lysate after centrifugation at 600 **g** for 10 min at 4 °C. Post-nucleus supernatant (PNS) was then spun sequentially at 3000, 4800, 15 000, 100 000 and 161 000 **g**. After each spin, supernatant was used for next centrifugation and pellet was dissolved in 15 μl of PMEE-IS buffer + 0.5% Igepal CA-630 (Rhodia, La Défense, France). The wall of centrifuge tube was wiped with cotton bud after each spin to minimise contamination of the pellet with the supernatant. The markers of the plasma membrane, endoplasmic reticulum, Golgi complex, and heavy and light-density vesicles were detected by immunoblotting. Differential centrifugation was performed twice per condition.

Immunoblotting

Proteins in the cytosols extracted from N11 cells and mouse hypothalamus and in the samples of immunoprecipitation and differential centrifugation were boiled with SDS loading buffer, separated in NuPAGE 4–11% Bis-Tris protein gels (Life Technologies), transferred to nitrocellulose membrane (Protran® BA-85, 0.45 μm; Whatman-GE Healthcare Life Science, Piscataway, NJ, USA) and detected by immunoblotting using primary antibodies.

Statistical analysis

All experiments were replicated multiple times with different batches of cell cultures. Microscopic analysis was performed by students blinded to the experimental set-up. Statistical significance between two groups was calcu-

lated using unpaired Student's t-test. $P < 0.05$ was considered statistically significant. Multiple comparisons were performed using one-way ANOVA followed by Dunnett's multiple comparisons test (GraphPad Prism software, La Jolla, CA, USA).

Results

The antibody 4660 specifically recognises ANXA1 in mouse hypothalamus and immortalised oxytocin neurones

We have studied about the role of snapin (47) in microtubule-based transport of vesicles containing pro-opiomelanocortin, the precursor of the stress hormone, adrenocorticotrophin, in the anterior pituitary AtT20 cells (in preparation). We generated two different batches of chicken antibodies (4659 and 4660) against the recombinant protein of full-length snapin. The antibody 4659 recognised 15-kDa snapin and other proteins in the cytosols of AtT20 cells. Snapin in AtT20 cells was also recognised by rabbit anti-snapin antibody (PTG10055-2-AP; Proteintech Group, Inc. Chicago, IL, USA; Fig. 1A). Conversely, the antibody 4660 recognised only the 38-kDa protein in the cytosols of AtT20 cells. To examine whether snapin exists in the hypothalamus and oxytocin neurones, we probed the cytosols extracted from mouse hypothalamus and immortalised oxytocin neurones (N11 cells) with the antibodies 4659 and 4660. The antibody 4659 did not recognise either 15-kDa snapin or 38-kDa protein in mouse hypothalamus and N11 cells, whereas the antibody 4660 recognised only the 38-kDa protein (Fig. 1B). We precipitated the 38-kDa protein in the cytosol of N11 cells by immunoprecipitation using antibody 4660 and sent the 38-kDa protein to the Department of Chemistry at the University of Kentucky for peptide sequencing. The amino acid sequence of the 38-kDa protein matched 100% to that of ANXA1 but < 13% to snapin according to EXPASY alignment program 'lalign' (http://www.expasy.org/). We confirmed the identity of the 38-kDa protein band in the cytosol of N11 cells using mouse anti-ANXA1 antibody (sc-12740) from Santa Cruz Biotechnology (Fig. 1B,C). Of note, mouse anti-ANXA1 antibody also recognised two other unknown proteins of approximately 40 kDa and 15 kDa in addition to 38 kD ANXA1 in the cytosol extracted from the mouse hypothalamus. We also confirmed that the 4660 antibody specifically recognised recombinant ANXA1 protein tagged with glutathione-*s*-transferase [GST-ANXA1: molecular weight = 64.6: 26.6 (GST) + 38 (ANXA1)] but not GST tag alone (Fig. 1D). The 4660 antibody also recognised a cleavage product (approximately 58 kDa) of GST-ANXA1 that might be generated during GST pulldown experiment. Mouse anti-ANXA1 antibody recognised GST-ANXA1 well but not GST alone (Fig. 1D). Although it is possible that both 4659 and 4660 antibodies may react with an epitope of the amino acid sequence that is similar to snapin and ANXA1, the antibody 4660 could not maintain its binding to the amino acid sequence of snapin with our stringent washing conditions using 0.1% Tween 20. We used antibody 4660, which recognised only ANXA1 in the mouse hypothalamus and immortalised oxytocin neurones to detect and precipitate endogenous ANXA1 in N11 cells and mouse hypothalamic neurones for the present study.

ANXA1 colocalises with oxytocin-containing vesicles in the processes of N11 cells and along the axons of primary oxytocin neurones

Given that the majority of ANXA1 associates with large dense core vesicles (LDCVs) in endocrine cells (42), it is possible that ANXA1 associates with oxytocin-containing LDCVs in hypothalamic neurones. We examined this possibility by immunostaining N11 cells and primary mouse oxytocin neurones (E17, DIV14) cultured on poly-L-

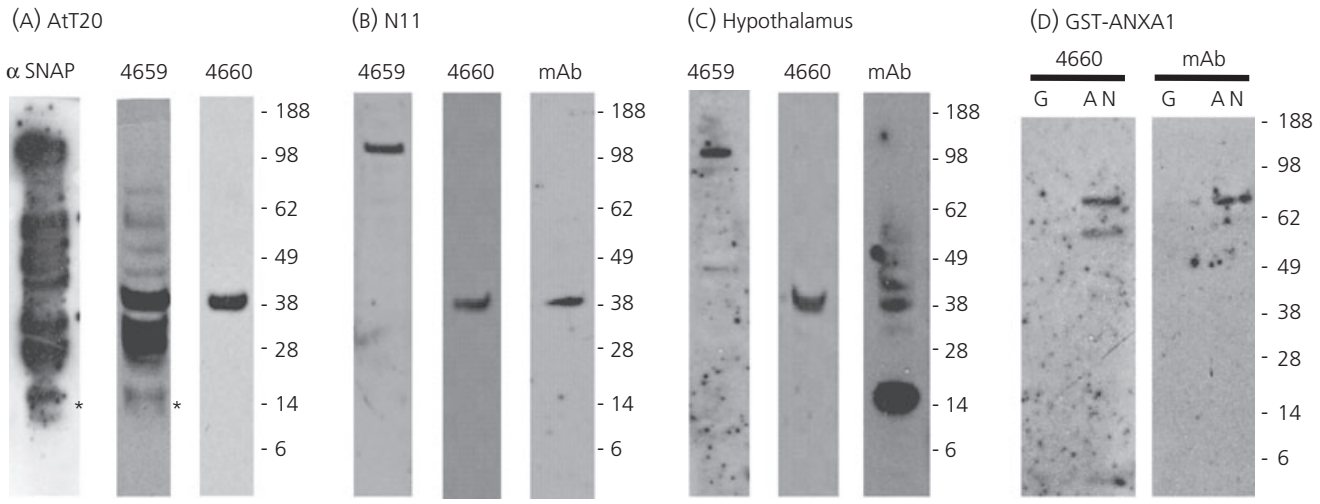

Fig. 1. The antibody 4660 recognises specifically annexin A1 (ANXA1) in AtT20 and N11 cells and mouse hypothalamus. Proteins in the cytosols (5 mg/ml) extracted from AtT20 cells (A), untransfected N11 cells (B) and mouse hypothalamus tissues (C) were detected by immunoblotting. Anti-snapin rabbit antibody (αSNAP) and two chicken antibodies (4659 and 4660) were used to detect 15-kDa snapin (marked with an asterisk '*') and a 38-kDa protein (ANXA1) in AtT20 cells (A). The antibodies 4659 and 4660 and mouse anti-ANXA1 antibody (mAb) were used to detect ANXA1 in N11 cells (B) and in mouse hypothalamus (C). (D) The antibody 4660 and mouse anti-ANXA1 antibody (mAb) were used to detect recombinant ANXA1 protein tagged with glutathione-*S*-transferase (GST) (GST-ANXA1: *AN*) and GST tag alone (*G*) that were purified from bacteria.

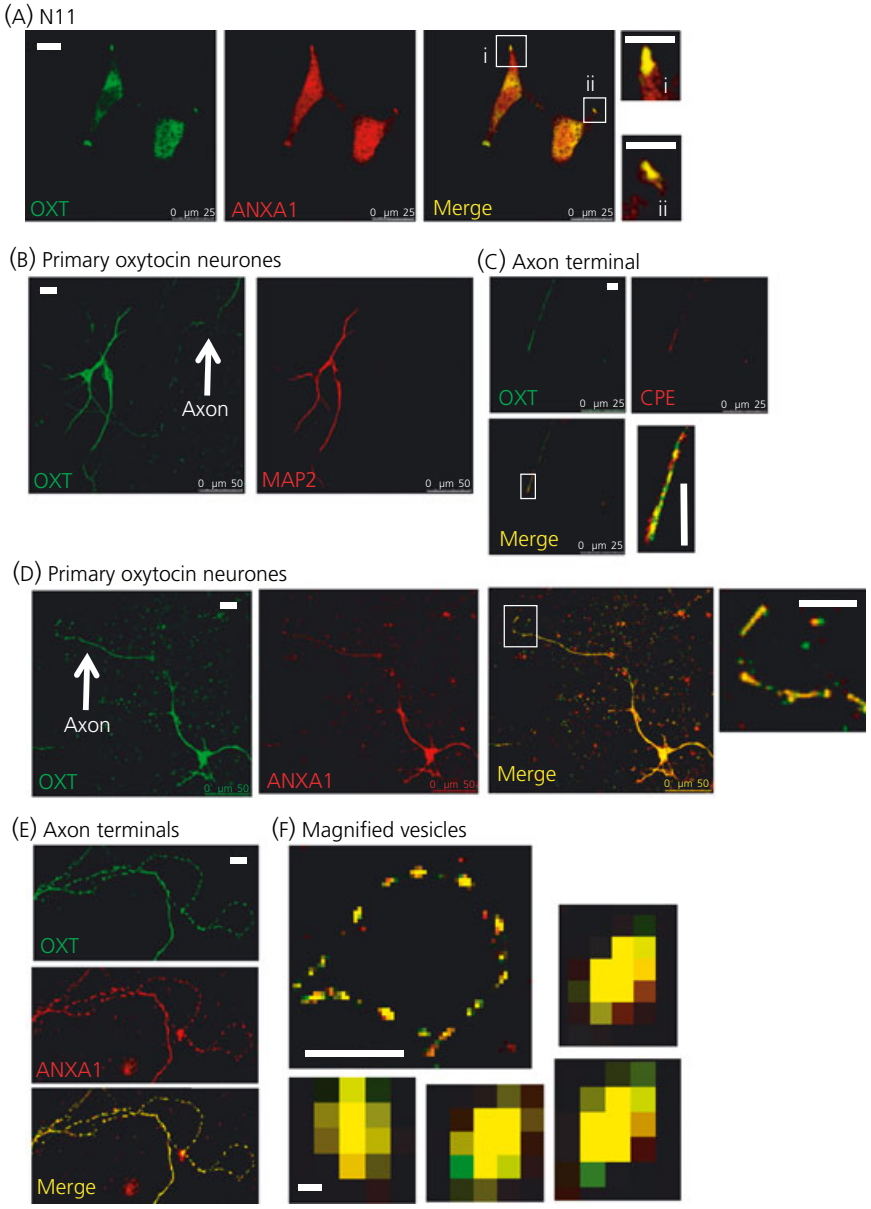

Fig. 2. Annexin A1 (ANXA1) colocalises with oxytocin vesicles (OXT) at the process tips of N11 cells and in the axons of primary hypothalamic neurones. (A) N11 cells grown on poly-L-lysine-coated coverslips were processed for immunocytochemistry with antibodies to oxytocin (green) and ANXA1 (red). Scale bars = 10 μm. (B–E) Primary mouse hypothalamic neurones at gestation day 17 (E17) were differentiated on poly-L-lysine-coated coverslips in neurobasal/B27 medium for 14 days (DIV14) and processed for immunocytochemistry with antibody to microtubule-associated protein 2 (MAP2) (B), carboxypeptidase E (CPE) (C) or ANXA1 (D–F) along with anti-oxytocin antibody. (B) Primary oxytocin neurones formed a long axon that was not stained by anti-MAP2 antibody. (C) The image of oxytocin vesicles and CPE at the axon terminals of the neurones was taken by confocal microscope. Scale bars = 5 μm. The inset of panel (D) shows the co-localisation of oxytocin vesicles with ANXA1 in the axon. (D–F) ANXA1 showed significant co-localisation with vesicles containing oxytocin at the axon terminals. Scale bars = 10 μm. The insets of panel (F) show the overlapping between the green pixels of oxytocin and the red pixels of ANXA1. Scale bars of the insets = 0.13 μm (equivalent to the diameter of one pixel).

lysine-coated coverslips with primary antibodies to ANXA1 and oxytocin. In N11 cells, ANXA1 co-localised with oxytocin-containing vesicles accumulated at the process tips (Fig. 2A). We quantified the correlation co-efficient of co-localisation (CCC) (45) between ANXA1 and oxytocin vesicles using METAMORPH. The CCC between ANXA1 and oxytocin vesicles in the processes reached 0.80 ± 0.01 (mean ± SEM, n = 40 cells), indicating significant co-localisation.

Primary oxytocin neurones formed long thin axons negative for MAP2 and thick dendrites positive for MAP2 (Fig. 2B). To examine whether LDCVs containing CPE, a LDCV marker, co-localise with oxytocin in the axons, we stained primary hypothalamic neurones with anti-CPE and anti-oxytocin antibodies. CPE was very sparse along the axons of oxytocin neurones but rich in the cell bodies and dendrites of the neurones. At the axon terminals of untreated

oxytocin neurones, a small amount of CPE partially co-localised with oxytocin vesicles (Fig. 2C). It suggests that only a subpopulation of oxytocin-containing vesicles in the axon may have CPE.

There were distinguishable individual LDCVs containing oxytocin along thin axons (Fig. 2D–F). Meanwhile, we could not find distinguishable individual oxytocin vesicles in the cell body and dendrites (Fig. 2D). The oxytocin-containing LDCVs along the axons showed significant co-localisation with ANXA1 (Fig. 2E, mean ± SEM CCC = 0.71 ± 0.03; n = 40 neurones). To obtain more detailed information about the co-localisation between ANXA1 and oxytocin vesicles, we attempted to perform voxel co-localisation analysis, a method to quantify the extent of the overlapping of volumic pixels (voxels) between two different fluorescence colours. However, we could not measure voxels because it was not possible to take multiple images along the *z*-axis through the thin axons of oxytocin neurones. Instead, we calculated the percent of the overlapping of the green fluorescent pixels of oxytocin vesicle with the red fluorescent pixels of ANXA1 on the vesicle using METAMORPH (Fig. 2F). The mean ± SEM percentage of ANXA1-colocalising oxytocin pixels per vesicle was 70.4 ± 1.2% (n = 47 vesicles). Thus, it is clear that ANXA1 associates with oxytocin-containing LDCVs in the axons of primary hypothalamic oxytocin neurones.

ANXA1 mediates the anterograde transport of oxytocin vesicles along the axon via its interaction with kinesin-2

A previous study showed that knockout of ANXA1 blocked the anterograde transport of Shiga toxin (43), suggesting that ANXA1 may be involved in intracellular anterograde transport. We examined whether ANXA1 is required for the anterograde transport of oxytocin-containing LDCVs by knocking down ANXA1 in primary hypothalamic neurones using lentiviral shRNA against ANXA1. Primary hypothalamic neurones (E17, DIV14) were transduced with lentiviral particles containing either control or anti-ANXA1 shRNA for 5 days and processed for immunocytochemistry with antibodies to oxytocin and ANXA1. The mean ± SEM intensity of immunostained ANXA1 in neurones transduced with anti-ANXA1 lentiviral shRNA was decreased to approximately 26% (5.35 ± 0.37) of that (20.78 ± 1.33) in neurones transduced with control lentiviral shRNA (n > 50 neurones, P < 0.0001; Fig. 3A). Similarly, the mean intensity of immunostained oxytocin vesicles along the axons of neurones transduced with anti-ANXA1 lentiviral shRNA was significantly lower than that of neurones transduced with control lentiviral shRNA (n = 40 neurones; Fig. 3B,C). These results suggest that ANXA1 is required for the anterograde transport of oxytocin vesicles along the axons.

Given that ANXA1 is required for the anterograde transport of oxytocin vesicles along the axons, it is possible that ANXA1 interacts with kinesins, microtubule-based anterograde transporters. We performed co-immunoprecipitation using the antibody 4660 and the cytosols of mouse hypothalamus and N11 cells. ANXA1 interacted with kinesin-2 (KIF3A) but not with kinesin-1 (kinesin heavy chain) and kinesin-3 (KIF1A) in N11 cells and mouse hypothalamus (Fig. 4A,B). Thus, kinesin-2 appears to mediate the anterograde transport of oxytocin vesicles along the axons via its interaction with ANXA1. In addition to kinesin-2, ANXA1 interacted with the retrograde transporter, cytoplasmic dynein, and its activator, dynactin (Fig. 4A,B).

Activation of PKA enhances the anterograde transport of oxytocin vesicles to the axon terminals

Given that pharmacological treatments that activate PKA enhance oxytocin secretion at the axon terminals (18–21), activation of PKA may increase the anterograde transport of oxytocin vesicles to the axon terminals for secretion. To examine this possibility, we treated primary hypothalamic neurones with forskolin, which increases the intracellular level of cyclic AMP, an activator of PKA, and then quantified the intensity of immunostained oxytocin vesicles along the axons and at the axon terminals. Mouse hypothalamic neurones (E17, DIV14) were treated with either DMSO or 10 μM forskolin for 10, 20 and 30 min and immunostained using antibodies to oxytocin and ANXA1 (n = 40 neurones per each condition, two independent experiments). The mean intensity of oxytocin vesicles in the axons was gradually increased by longer period of incubation with forskolin (Fig. 5). The mean intensities of oxytocin vesicles in neurones treated with DMSO were approximately 20 (in arbitrary units) in the cell bodies, 10–15 in the axons between 0 and 100 μm from the cell body, and seven in those between 100 and 200 μm. After 10- and 20-min treatments with forskolin, the mean intensity of oxytocin vesicles in the cell body was decreased from approximately 20 (0 min) to 8 (10 min) and 8 (20 min; Fig. 5). Meanwhile, the mean intensities of oxytocin vesicles were increased to 20–22 in the axon between 0 and 100 μm and to 13–16 between 100 and 200 μm (Fig. 5B,C,E). At 30 min after forskolin treatment, the mean intensity of oxytocin vesicles in the axon was significantly increased to approximately 30, 26, 21 and 20 in axons between 0–50, 50–100, 100–150 and 150–200 μm, respectively. We specified the involvement of PKA in the enhancement of the axon-localisation of oxytocin vesicles by pre-treating neurones with 10 μM PKI-ester, a PKA inhibitor, for 1 h before 30 min of forskolin treatment. Pre-treatment with PKI-ester blocked forskolin from enhancing the axon-localisation of oxytocin vesicles (Fig. 5D). The mean intensities of oxytocin vesicles in the cell bodies and the axons of neurones pre-treated with PKI and forskolin were similar to those of neurones treated with DMSO (data not shown). In addition, we assessed the extents of co-localisation between oxytocin vesicles and ANXA1 along the axon during 30 min of stimulation with forskolin. ANXA1 maintained high levels of co-localisation with oxytocin vesicles (mean ± SEM CCC = 0.73 ± 0.01; n = 60) in the axons during 30 min of stimulation by forskolin.

We also quantified the mean intensities of oxytocin vesicles at the axon terminals of neurones treated with either DMSO or 10 μM forskolin for 30 min. The mean intensity of oxytocin vesicles at the axon terminals of forskolin-treated neurones was approximately three-fold higher than that of DMSO-treated neurones (n > 70 axon terminals; Fig. 6A,B,D).

All of these results suggest that activation of PKA enhances the anterograde transport of oxytocin vesicles along the

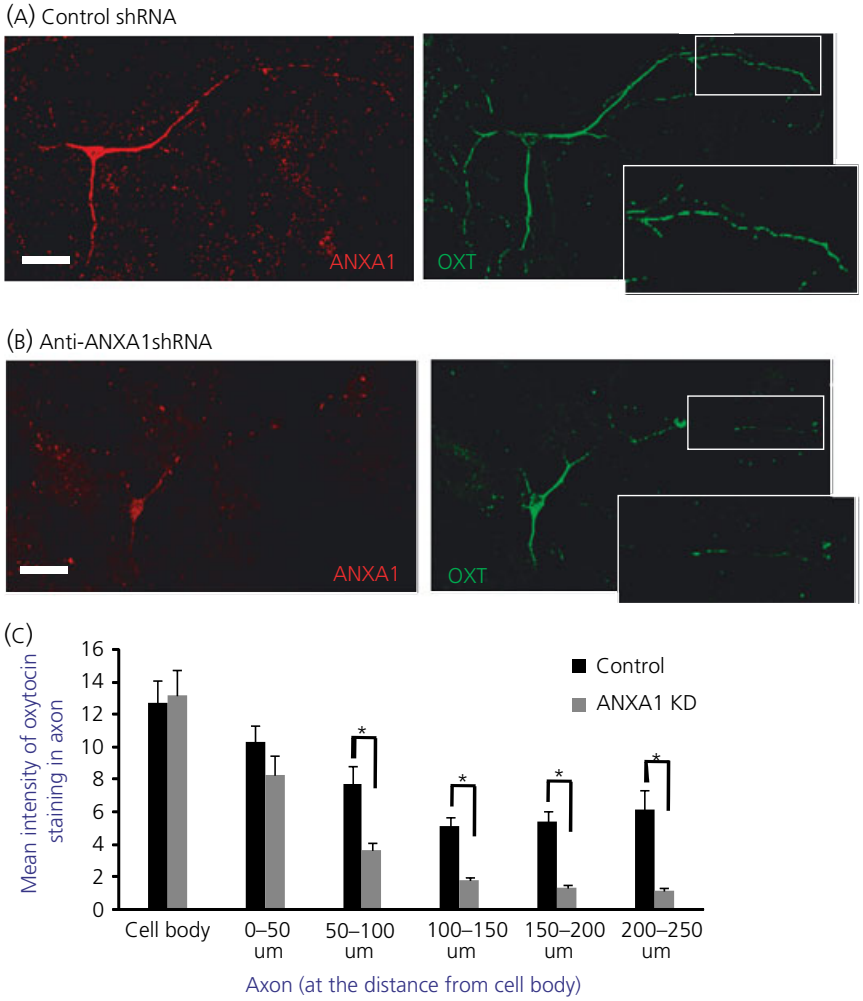

Fig. 3. Annexin A1 (ANXA1) is required for the axon-localisation of oxytocin vesicles (OXT) in primary hypothalamic neurones. Primary mouse hypothalamic neurones at gestation day 17 (E17) differentiated on poly-L-lysine-coated coverslips were transduced with control or anti-ANXA1 short hairpin (sh)RNA lentiviral particles for 5 days. Transduced neurones were then processed for immunocytochemistry using antibodies to ANXA1 (red) and oxytocin (green). The insets showed that neurones transduced with anti-ANXA1 shRNA (B) had low levels of ANXA1 and oxytocin vesicles in the axons compared to those transduced with control shRNA (A). Scale bars = 10 μm. (C) Bar graphs show the mean ± SEM intensities of oxytocin vesicles in the cell bodies and the axons between 0–50, 50–100, 100–150, 150–200 and 200–250 μm from the cell body of neurones transduced with either control or anti-ANXA1 shRNA (ANXA1 KD) (*$P < 0.001$).

axons, thus accumulating more oxytocin vesicles at the axon terminals.

Activation of PKA increases the association of kinesin-2 and AKAP150 with ANXA1

Because kinesins are the anterograde transporters that carry proteins and vesicles toward the axon terminals (48), it is possible that activation of PKA recruits more kinesins to oxytocin vesicles, thus enhancing the anterograde transport of the vesicles. Possibly, activation of PKA increases the binding of kinesins to ANXA1, a protein associated with oxytocin vesicles. We therefore performed co-immunoprecipitation using the antibody 4660 and the cytosols extracted from N11 cells treated with either DMSO or 10 μM forskolin for 30 min. Activation of PKA did, indeed, increase the association of kinesin-2 with ANXA1 compared to control (Fig. 4C). Conversely, activation of PKA had no effect on the binding of cytoplasmic dynein, dynactin, kinesin-1 and kinesin-3 to ANXA1. We also examined the effect of forskolin treatment on the association of AKAP150, a scaffold protein that targets the action of PKA to its associated proteins, with ANXA1. In untreated N11 cells and mouse hypothalamus, there was a basal level of interaction between AKAP150 and ANXA1 (Fig. 4A,B). The basal interaction between AKAP150 and ANXA1 was also observed in the counter pulldown by anti-dynactin antibody (Fig. 4E). Upon forskolin treatment, more AKAP150 was associated with ANXA1 (Fig. 4C). Thus, activation of PKA increases the binding of kinesin-2 to ANXA1, which should increase the anterograde transport of oxytocin vesicles. Increased binding of AKAP150 to ANXA1 may concentrate the action of PKA on oxytocin vesicles, thus enhancing the anterograde transport of the vesicles.

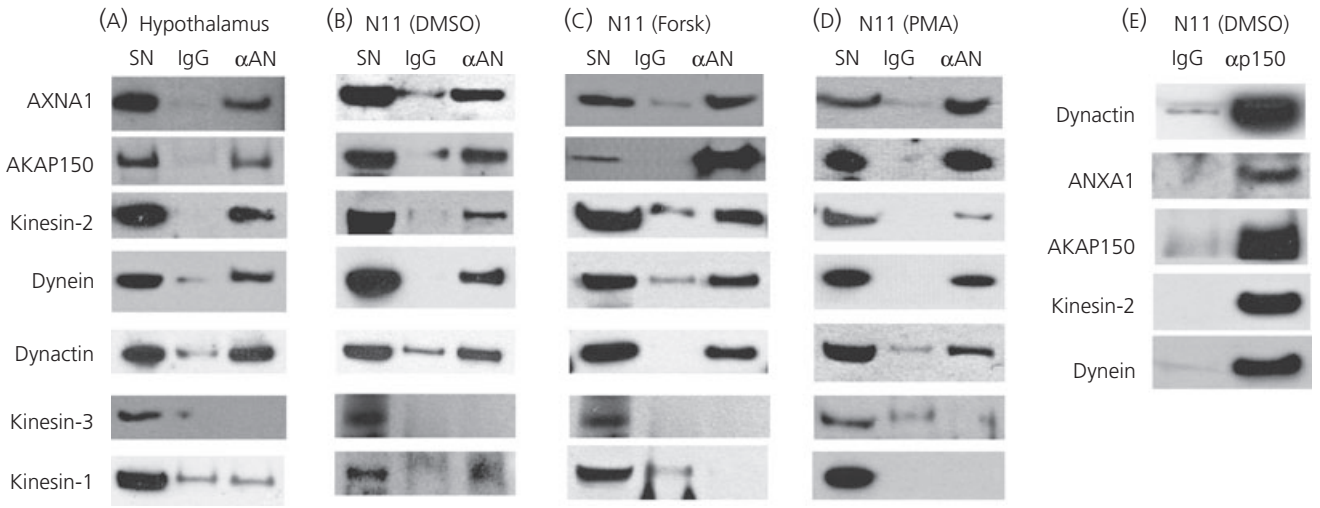

Fig. 4. Annexin A1 (ANXA1), A-kinase anchor protein 150 (AKAP150) and microtubule motors form a complex in mouse hypothalamus and N11 cells. The cytosols (5 mg/ml) of mouse hypothalamus tissues (A) or N11 cells (B–D) that were treated with dimethyl sulphoxide (B), 10 μM forskolin (C, Forsk) or 10 nM phorbol 12-myristate 13-acetate (PMA) (D) were mixed with the antibody 4660 along with protein A beads (60 μl) at 4 °C for 24 h. Proteins pulled down by anti-ANXA1 antibody (αAN) were probed by immunoblotting. (E) The cytosols [5 mg/ml, post-nuclear supernatant (SN)] of N11 cells were mixed with anti-p150 (dynactin) antibody for co-immunoprecipitation. Proteins bound to dynactin were detected by immunoblotting.

Activation of PKC decreases the binding of kinesin-2 to ANXA1, which may attenuate the anterograde transport of oxytocin vesicles

Previous studies suggest that activation of PKC may enhance somatodendritic oxytocin secretion but attenuate axonal secretion (16,23). Hence, we examined the effect of PKC on the axon-localisation of oxytocin vesicles and the interaction of ANXA1 with kinesin-2 and other proteins. Primary hypothalamic neurones (E17, DIV14) were treated with either DMSO or 10 nM phorbol ester (PMA) and immunostained with antibodies to oxytocin and ANXA1. The mean ± SEM intensities of oxytocin (4.71 ± 0.46) and ANXA1 (6.75 ± 0.58) in the axons of neurones treated with PMA (Fig. 6F,G) were similar to those of neurones treated with DMSO (oxytocin = 7.1 ± 0.7 and ANXA1 = 6.9 ± 0.6; n = 60 neurones; Fig. 6E,G). This finding suggests that PKC activation does not enhance the axon-localisation of oxytocin vesicles. We also quantified the mean intensity of oxytocin vesicles at the axon terminals of neurones treated with either DMSO or 10 nM PMA for 30 min. The mean intensity of oxytocin vesicles at the axon terminals of PMA-treated neurones was not different from that of DMSO-treated neurones (n > 70 axon terminals, P > 0.05; Fig. 6A,C,D). Next, we performed co-immunoprecipitation using the antibody 4660 and the cytosols extracted from N11 cells treated with either DMSO or 10 nM PMA. Activation of PKC did not affect the association of cytoplasmic dynein, dynactin, and AKAP150 with ANXA1 but decreased the binding of kinesin-2 to ANXA1 (Fig. 4D). The binding of kinesin-1 and kinesin-3 to ANXA1 was not affected by activation of PKC. These results suggest that activation of PKC may attenuate the anterograde transport of oxytocin vesicles along the axon by decreasing the association of kinesin-2 with oxytocin vesicles.

Activation of PKA increases the association of kinesin-2 and AKAP150 with light-density vesicles

We performed differential centrifugation to examine the effect of PKA and PKC on the association of ANXA1, AKAP150 and microtubule motors with LDCVs in N11 cells. N11 cells treated with DMSO, 10 μM forskolin or 10 nM PMA were processed to obtain cytosols (1 mg/ml) in 0.3 ml of PMEE buffer (49) + protease/phosphatase inhibitors + 0.25 M sucrose. PNS was obtained by spinning cell lysates at 600 **g**. PNS was spun sequentially at 3000, 4800, 15 000, 100 000 and 161 000 **g** to separate different membranous compartments. The plasma membrane (syntaxin-1), Golgi complex (p115) and endoplasmic reticulum (ER: calreticulin) were pelleted at 3000, 4800 and 15 000 (Fig. 7A). CPE, a heavy-density LDCV protein that travels from the ER through the Golgi complex to the plasma membrane (50), was found in the ER, Golgi complex, plasma membrane and heavy-density vesicle pool, and to a lesser extent in the light-density vesicle pool. Synaptophysin (SYN), a light-density vesicle marker, was pelleted at 161 000 and to some extent at 3000. Oxytocin-containing intermediates (15, 20–28, 34 kDa) were pelleted at 100 000 and 161 000, suggesting that there are two different-density LDCVs containing oxytocin. Two different-density oxytocin vesicles were also found in the mouse hypothalamus (Fig. 7D). We could not detect the mature form (nine amino acids, < 1 kD) of oxytocin because the nitrocellulose membrane (pore size = 0.45 μm) that we used could not hold peptides smaller than 2 kDa. Given that oxytocin vesicles in the axon contain a little CPE (Fig. 2C), it appears that light-density vesicles containing oxytocin and a little CPE (Fig. 7A) are targeted to the axon.

In untreated N11 cells, most ANXA1 was found in the heavy membrane fractions pelleted at 3000 and 4800 and the cytosol,

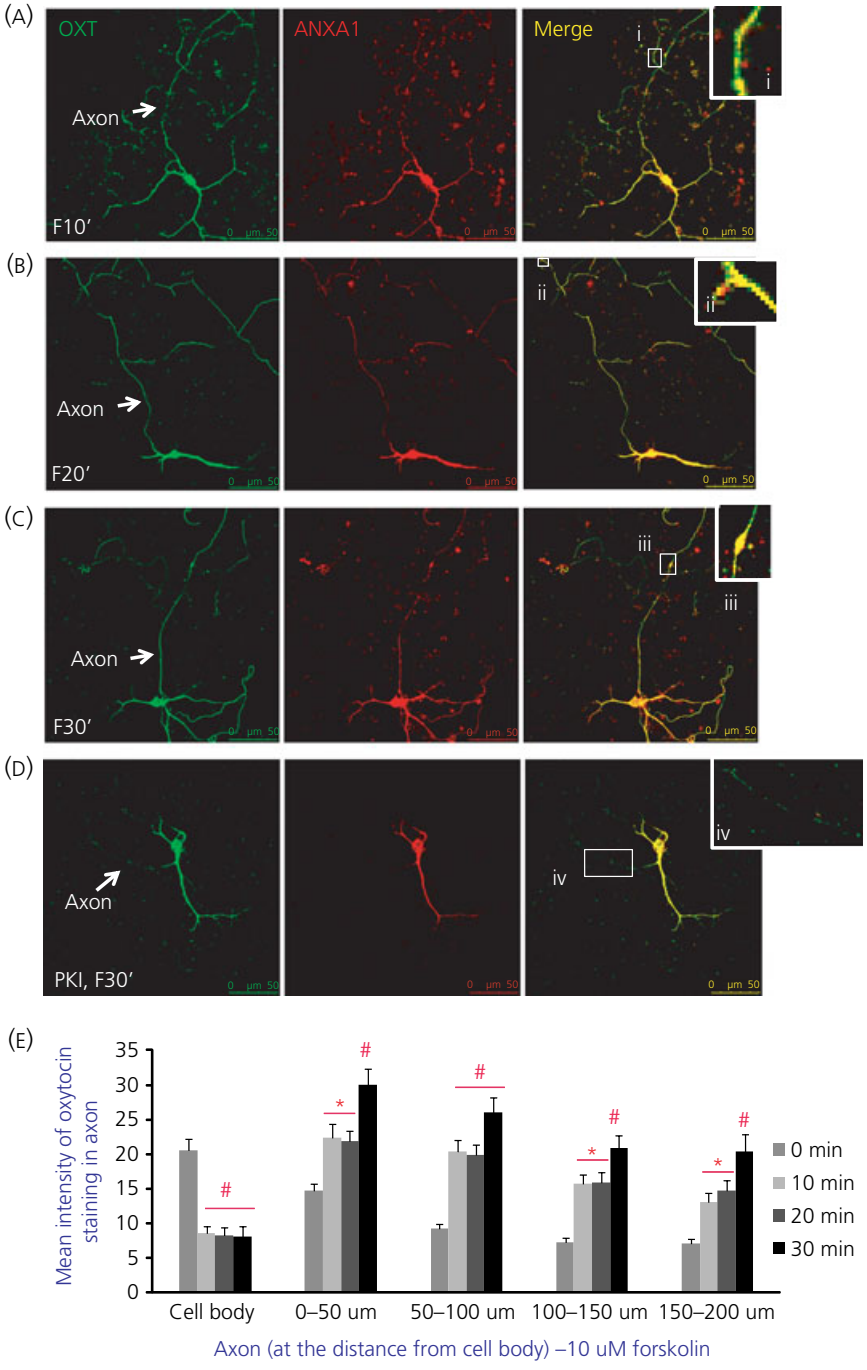

Fig. 5. Vesicles containing oxytocin (OXT) and annexin A1 (ANXA1) co-migrate toward the axon terminal in response to protein kinase A (PKA) activation. Mouse hypothalamic neurones (E17, DIV14) were treated with dimethyl sulphoxide or 10 μM forskolin for 10 min (A, F10′), 20 min (B, F20′), and 30 min (C, F30′) and stained using antibodies to oxytocin and ANXA1. The axons are indicated by arrows. The magnified images in the insets show the co-localisation between oxytocin and ANXA1 at the distal axons of neurones treated with forskolin for 10 min (inset i), 20 min (inset ii) and 30 min (inset iii). Scale bar = 50 μm. (D) To specify the involvement of PKA in forskolin-induced axon-localisation of oxytocin vesicles, neurones were pretreated with 10 μM PKI-ester for 1 h before 30 min of forskolin treatment (inset iv). (E) The mean intensities of oxytocin vesicles in cell bodies and along axons (0–50, 50–100, 100–150 and 150–200 μm) were quantified using METAMORPH (n = 30 per condition). Bar graphs show the mean ± SEM intensities of oxytocin vesicles along the axons (0–50, 50–100, 100–150 and 150–200 μm) of neurones treated with forskolin (0, 10, 20 and 30 min) (#P < 0.0001, *P < 0.01 compared to control).

whereas a small amount of ANXA1 was pelleted at 15 000, 100 000 and 161 000 (Fig. 7A). Conversely, in forskolin-treated N11 cells, the amount of ANXA1 that was associated with light-density vesicles was increased (Fig. 7B). In PMA-treated N11 cells, ANXA1 was found in all the fractions (Fig. 7C). Kinesin-2 was found mostly in the vesicle pools and cytosol of untreated N11 cells. Treatment

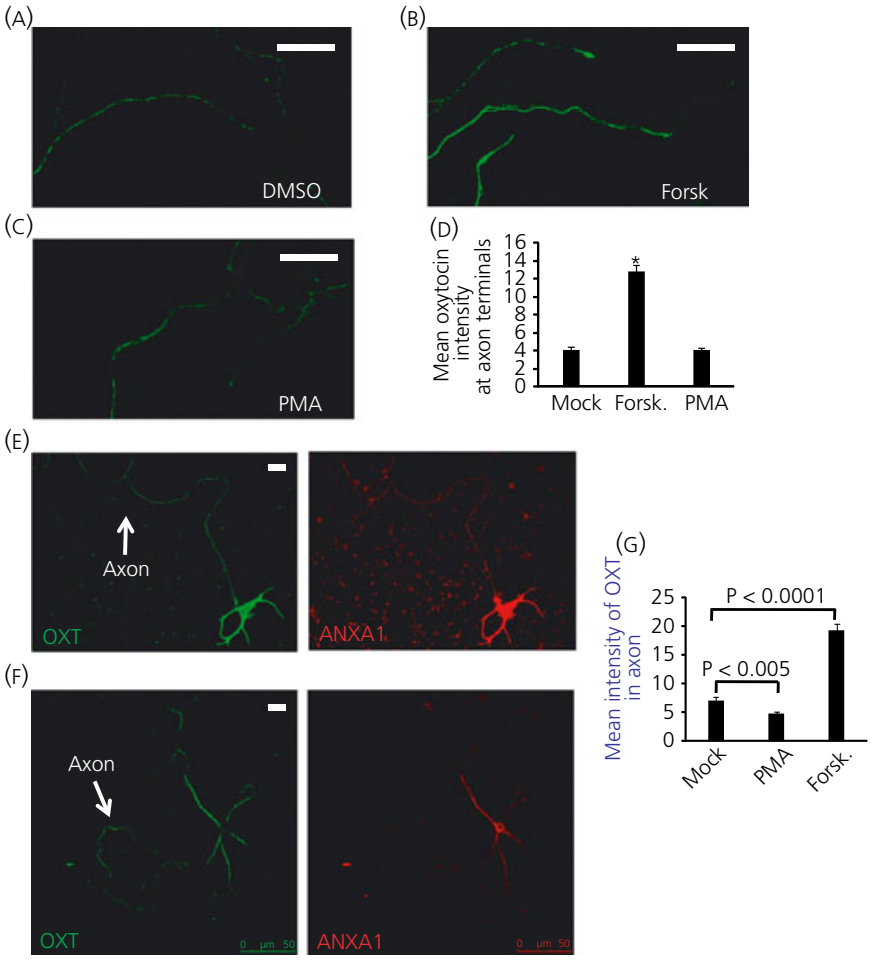

Fig. 6. Activation of protein kinase A (PKA) increases the localisation of oxytocin-containing vesicles (OXT) to axon terminals, whereas that of protein kinase C (PKC) decreases it. Mouse hypothalamic neurones (E17, DIV14) were treated with dimethyl sulphoxide (DMSO) (A), 10 μM forskolin (B, Forsk) or 10 nM phorbol 12-myristate 13-acetate (PMA) (C) for 30 min and stained using anti-oxytocin antibody. The images of oxytocin vesicles at the axon terminals of the neurones were taken by confocal microscope. Scale bars = 10 μm. (D) Bar graphs show the mean ± SEM intensities of oxytocin vesicles at the axon terminals of neurones treated with DMSO, forskolin or PMA (*P < 0.01). (E,F) Mouse hypothalamic neurones treated with DMSO (E) or PMA (F) were stained using antibodies to oxytocin and ANXA1. The axons were indicated by arrows. Scale bars = 10 μm. (G) Bar graphs show the mean ± SEM intensities of oxytocin vesicles in the axons of neurones treated with DMSO, PMA and forskolin (Forsk.). (n = 60 neurones per condition; *P < 0.001: DMSO versus forskolin).

with forskolin increased the association of kinesin-2 with light-density vesicles (Fig. 7B), whereas that with PMA decreased the association of kinesin-2 even with heavy-density vesicles (Fig. 7C). AKAP150 was found mostly in the light-density vesicles and cytosols of cells when the cells were treated with forskolin (Fig. 7B), whereas it was in all the fractions of cells treated with either DMSO (Fig. 7A) or PMA (Fig. 7C). The association of cytoplasmic dynein, dynactin and kinesin-1 with heavy- and light-density vesicles was not changed by treatment with either forskolin (Fig. 7B) or PMA (Fig. 7C). These results suggest that activation of PKA increases the association of kinesin-2 with light-density oxytocin vesicles that contain oxytocin and a little CPE, thus enhancing the anterograde transport of the vesicles to the axon. Conversely, activation of PKC that decreases the association of kinesin-2 with ANXA1 on oxytocin vesicles may block the anterograde transport of oxytocin vesicles to the axon.

Discussion

Oxytocin is a major socialising neuropeptide in the brain (51). Oxytocin secreted from the somatodendritic regions of the hypothalamic neurones activates its receptors in the hypothalamus and the brain regions neighbouring the hypothalamus (1,2). Some oxytocin travels along the long axon to the distal brain regions such as septum, substantia nigra, stria terminalis, olfactory bulb, brainstem and spinal cord (7–14). Brain oxytocin modulates brain functions involved in behaviour, anxiety, cognition and autonomic nerve activity (15). Oxytocin is also secreted from the axons that innervate the posterior pituitary gland into the blood circulation, thus increasing natriuresis and reducing blood pressure and heart rate (3–6). There appears to be a 'yin and yang' mechanism for controlling the distribution of oxytocin secretion between the axon and the somatodendritic region. Extracellular stimuli that activate PKA

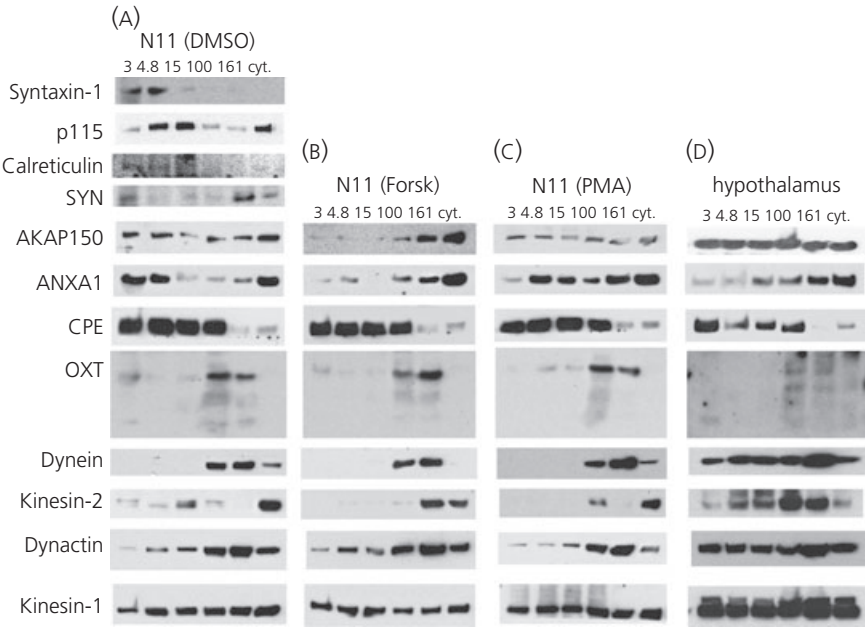

Fig. 7. Activation of protein kinase A (PKA) increases the association of kinesin-2 with light-density vesicles. (A–D) Post-nucleus supernatant was obtained from either N11 cells [treated with dimethyl sulphoxide (A), 10 μM forskolin (B) or 10 nM phorbol 12-myristate 13-acetate (C)] or mouse hypothalamus tissues (D) by spinning cell or tissue extracts at 600 **g** to remove nuclei and cell debris. Post-nucleus supernatant was spun sequentially at 3000, 4800, 15 000, 100 000 and 161 000 **g**. The pellet after each spin was re-suspended in 0.5% Igepal CA-630-containing PMEE to extract proteins from lipid membrane. Proteins in the pellets and cytosol (cyt.) were detected by immunoblotting. Markers for plasma membrane (syntaxin-1), p115 (Golgi complex), calreticulin (ER), CPE (heavy density vesicles), synaptophysin (SYN: light density vesicles) and oxytocin (OXT) in the pellets and cytosol were detected by immunoblotting.

enhance the secretion of oxytocin at the axon terminals (18–21), whereas those that activate PKC enhance somatodendritic oxytocin secretion and attenuate oxytocin secretion at the axon terminal (16,22,23). Thus far, the molecular mechanism underlying the regulation of the distribution of oxytocin vesicles for secretion between the axon and the somatodendritic region remains largely unknown.

We have discovered that ANXA1 forms a complex with AKAP150, a protein that interacts with PKA and PKC (24–28), and microtubule motors in the hypothalamus and immortalised oxytocin neurones. Pixel analysis of the co-localisation between ANXA1 and oxytocin vesicles clearly shows that ANXA1 associates with oxytocin-containing LDCVs in the axons of primary oxytocin neurones. The interaction of ANXA1 complex with kinesin-2, an anterograde transporter, is modified differently by PKA and PKC. Activation of PKA increases the binding of kinesin-2 to ANXA1, which appears to enhance the anterograde transport of oxytocin vesicles toward the axon terminals. Conversely, activation of PKC decreases the binding of kinesin-2 to ANXA1, which may decrease the axon-localisation of oxytocin vesicles. Thus, our results indicate that PKA and PKC determine the directionality of oxytocin vesicle movements in the axon by controlling the binding of kinesin-2 to ANXA1 on oxytocin vesicles (Fig. 8).

Our finding of a new molecular mechanism by which the directionality of vesicle movements is controlled should provide new insight into peptidergic vesicle trafficking in endocrine and neuroendocrine cells. As reviewed recently (48), even the molecular mechanism by which peptidergic vesicles are transported along microtubules in peptidergic neurones and endocrine cells is not fully understood. KIF1A mediates the anterograde transport of peptidergic vesicles in *Caenorhabditis elegan* (52). A microtubule motor complex consisting of kinesin-2, cytoplasmic dynein and dynactin mediates the bi-directional movement of stress hormone vesicles in AtT20 cells (49). A similar complex mediates the transport of vesicles containing brain-derived neurotrophic factor in hippocampal neurones (53) with the assistance of Htt-associated protein-1 (54, 55). In premature neurones, bicaudal-D-related protein 1 mediates peptidergic vesicle transport required for neurite outgrowth by interacting simultaneously with Rab6 on LDCVs and with a motor complex consisting of dynactin, cytoplasmic dynein and kinesin-3 (56). We speculate that ANXA1 complex may coordinate the actions of PKA and/or PKC in those transport systems, thus determining the direction of hormone vesicle movements to different secretion sites (e.g. the axon versus the cell body).

Is the binding of more kinesin-2 to vesicles sufficiently strong to push the vesicles toward the anterograde direction? Under resting conditions, bi-directional microtubule-based transport is nearly at force balance between a small group of strong torque kinesins and a large team of weak torque cytoplasmic dynein (57–59). A single kinesin competes with at least five cytoplasmic dyneins for changing the direction of microtubule-based transport (59). Thus, the directionality of microtubule-based transport is determined by either the association/dissociation of a single strong torque kinesin or the number of multiple weak torque cytoplasmic dyneins. Therefore, the increase in the association of kinesin-2 with ANXA1 on oxytocin vesicles without affecting that of cytoplasmic dynein should push oxytocin vesicles toward the axon terminals of neuro-

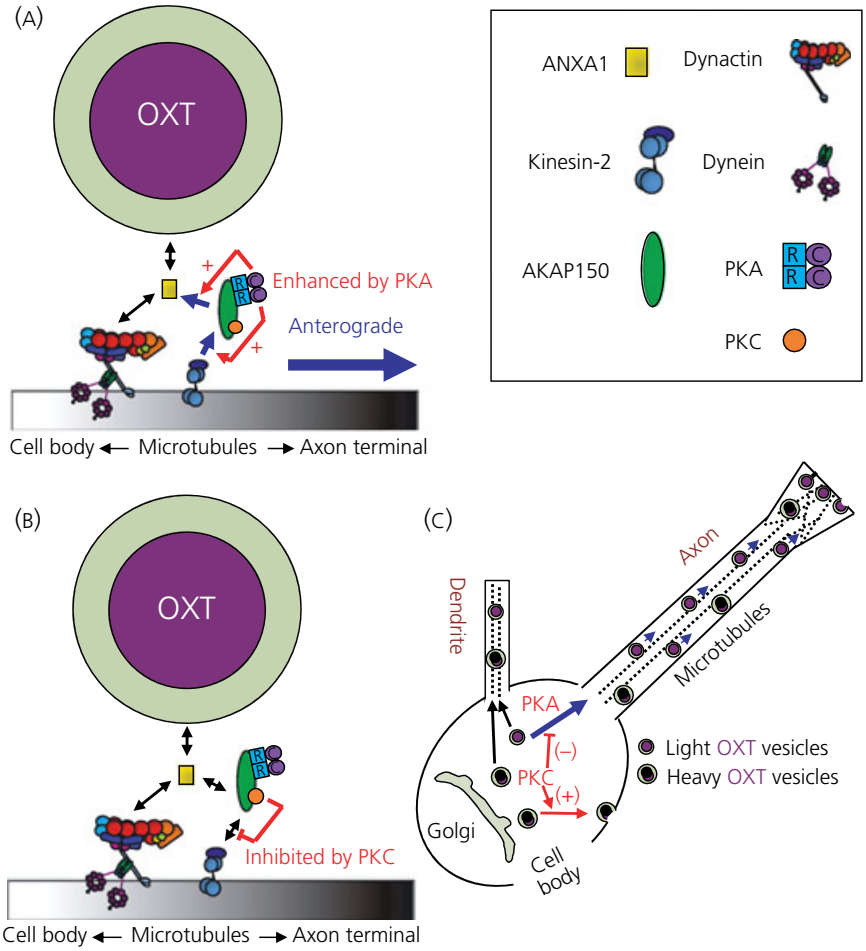

Fig. 8. Schematic illustration of how protein kinase A (PKA) and protein kinase C (PKC) affect the interaction of annexin A1 (ANXA1) with A-kinase anchor protein 150 (AKAP150) and kinesin-2, thus changing the direction of movement of oxytocin-containing vesicles. (A) Upon activation of PKA that consists of two catalytic [*C*] and two regulatory [*R*] subunits, the regulated subunits withdraw their inhibitory action from the catalytic subunits. Then, the catalytic subunits increase the binding of kinesin-2 and AKAP150 to ANXA1 on light-density oxytocin (OXT) vesicle without affecting the interaction of cytoplasmic dynein-dynactin with ANXA1, resulting in enhancement of anterograde transport of the vesicles to the axon terminal. (B) Activated PKC inhibits the interaction of kinesin-2 with AKAP150-ANXA1 complex without affecting the interaction of cytoplasmic dynein-dynactin with ANXA1 complex, resulting in inhibition of anterograde transport of oxytocin vesicles to the axon terminal. (C) Activation of PKA enhances the anterograde transport of light-density oxytocin vesicles to the axon terminals, whereas activation of PKC inhibits the anterograde transport. Activation of PKC increases somatic exocytosis of oxytocin vesicles. Some heavy density oxytocin vesicles are transported to the axon and dendrites.

nes treated with PKA activator. Conversely, the dissociation of kinesin-2 from ANXA1 on oxytocin vesicles in neurones treated with PKC activator should shift the direction of vesicle movement toward the cell body. This mechanism may be how extracellular stimuli adjust the amount of oxytocin for secretion at the axon terminal versus the somatodendritic region. It is possible that most peptidergic neurones with long axons such as hippocampal neurones use ANXA1-AKAP150-kinesin-2 complex or a similar complex to refill depleted secretion sites at the axon terminal quickly in a PKA-dependent manner for release of a proper amount of hormones in response to repetitive stimulation.

To clarify the difference of our finding of the association of ANXA1 with peptidergic vesicles with respect to the findings of a subset of previous studies (60, 61), we attempted to perform immuno-electron microscopy using primary hypothalamic neurones cultured *in vitro*, although it was found that this was not possible as a result of technical difficulties with respect to obtaining sections of the intact thin axons of hypothalamic primary neurones. Nonetheless, our high magnification images clearly show significant co-localisation of ANXA1 with oxytocin vesicles in the axon. Given that ANXA1 is expressed as an intracellular (not extracellular) protein (36) and found mostly on LDCVs in endocrine cells (42), it may reside on the extravesicular surface of oxytocin vesicles.

We observed the presence of two different-density oxytocin vesicles in immortalised N11 cells and mouse hypothalamus. Light-density vesicles appear to contain some CPE, an LDCV enzyme that removes the C-terminal bi-basic residues of pro-hormones (50). Most oxytocin vesicles in the axons may be light-density vesicles containing a little CPE. Additional studies are needed to further characterise these light-density oxytocin vesicles.

In conclusion, the findings of the present study demonstrate that ANXA1 forms a complex with AKAP150 and microtubule motors in the hypothalamus, specifically in oxytocin neurones. This complex coordinates the actions of PKA and PKC to control the direction of oxytocin vesicle movement by changing the association of the anterograde strong torque motor, kinesin-2, with oxytocin vesicles (Fig. 8). Our study reveals, for the first time, a novel molecular mechanism that peptidergic neurones use to control the microtubule-based transport of neuropeptide-containing vesicles to secretion sites. Further studies should help identify molecular targets for improving the treatments of endocrine and psychiatric disorders that are caused by abnormal hormone secretion.

Acknowledgements

We thank Dr Andrea Kalinoski (University of Toledo Microscopy Imaging Core) for technical support. We also thank Dr Y. Peng Loh for the 4659 and 4660 antibodies. This research was supported by NICHD K22 (1K22HD056137-01A1) and ARRA funding.

Received 4 March 2013,
revised 24 September 2013,
accepted 29 September 2013

References

1 Gimpl G, Fahrenholz F. The oxytocin receptor system: structure, function, and regulation. *Physiol Rev* 2001; **81**: 629–683.
2 Hirasawa M, Kombian SB, Pittman QJ. Oxytocin retrogradely inhibits evoked, but not miniature, EPSCs in the rat supraoptic nucleus: role of N- and P/Q-type calcium channels. *J Physiol* 2001; **532**: 595–607.
3 Lee HJ, Macbeth AH, Pagani JH, Young WS 3rd. Oxytocin: the great facilitator of life. *Prog Neurobiol* 2009; **88**: 127–151.
4 Gutkowska J, Jankowski M. Oxytocin revisited: its role in cardiovascular regulation. *J Neuroendocrinol* 2011; **24**: 599–608.
5 Petersson M. Cardiovascular effects of oxytocin. *Prog Brain Res* 2002; **139**: 281–288.
6 Soares TJ, Coimbra TM, Martins AR, Pereira AG, Carnio EC, Branco LG, Albuquerque-Araujo WI, de Nucci G, Favaretto AL, Gutkowska J, McCann SM, Antunes-Rodrigues J. Atrial natriuretic peptide and oxytocin induce natriuresis by release of cGMP. *Proc Natl Acad Sci USA* 1999; **96**: 278–283.
7 Buijs RM, deVries GJ, VanLeeeuwen FW. Distribution and synaptic release of oxytocin in the central nervous system. In: Amico JA, Robinson AG, eds. *Oxytocin: Clinical and Laboratory Aspects*. Oxford: Elsevier Science Publishers, 1985; **666**: 77–86.
8 Blevins JE, Eakin TJ, Murphy JA, Schwartz MW, Baskin DG. Oxytocin innervation of caudal brainstem nuclei activated by cholecystokinin. *Brain Res* 2003; **993**: 30–41.
9 Buijs RM, Van der Beek EM, Renaud LP, Day TA, Jhamandas JH. Oxytocin localization and function in the A1 noradrenergic cell group: ultrastructural and electrophysiological studies. *Neuroscience* 1990; **39**: 717–725.
10 Peters JH, McDougall SJ, Kellett DO, Jordan D, Llewellyn-Smith IJ, Andresen MC. Oxytocin enhances cranial visceral afferent synaptic transmission to the solitary tract nucleus. *J Neurosci* 2008; **28**: 11731–11740.
11 Llewellyn-Smith IJ, Kellett DO, Jordan D, Browning KN, Travagli RA. Oxytocin-immunoreactive innervation of identified neurons in the rat dorsal vagal complex. *Neurogastroenterol Motil* 2011; **24**: e136–e146.
12 Ingram CD, Moos F. Oxytocin-containing pathway to the bed nuclei of the stria terminalis of the lactating rat brain: immunocytochemical and in vitro electrophysiological evidence. *Neuroscience* 1992; **47**: 439–452.
13 Buijs RM, De Vries GJ, Van Leeuwen FW, Swaab DF. Vasopressin and oxytocin: distribution and putative functions in the brain. *Prog Brain Res* 1983; **60**: 115–122.
14 Nicholas AP, Hancock MB. Evidence for substance P, serotonin and oxytocin input to medullary catecholamine neurons with diencephalic projections. *Brain Res Bull* 1989; **22**: 213–223.
15 Barberis C, Tribollet E. Vasopressin and oxytocin receptors in the central nervous system. *Crit Rev Neurobiol* 1996; **10**: 119–154.
16 Sabatier N. Alpha-melanocyte-stimulating hormone and oxytocin: a peptide signalling cascade in the hypothalamus. *J Neuroendocrinol* 2006; **18**: 703–710.
17 Ludwig M, Sabatier N, Bull PM, Landgraf R, Dayanithi G, Leng G. Intracellular calcium stores regulate activity-dependent neuropeptide release from dendrites. *Nature* 2002; **418**: 85–89.
18 Galfi M, Radacs M, Juhasz A, Laszlo F, Molnar A, Laszlo FA. Serotonin-induced enhancement of vasopressin and oxytocin secretion in rat neurohypophyseal tissue culture. *Regul Pept* 2005; **127**: 225–231.
19 Osei-Owusu P, James A, Crane J, Scrogin KE. 5-Hydroxytryptamine 1A receptors in the paraventricular nucleus of the hypothalamus mediate oxytocin and adrenocorticotropin hormone release and some behavioral components of the serotonin syndrome. *J Pharmacol Exp Ther* 2005; **313**: 1324–1330.
20 Bojanowska E, Stempniak B. tGLP-1 and release of vasopressin and oxytocin from the isolated rat hypothalamo-neurohypophysial system: effects of a tGLP-1 receptor agonist and antagonist. *J Physiol Pharmacol* 2001; **52**: 781–793.
21 Onaka T. Neural pathways controlling central and peripheral oxytocin release during stress. *J Neuroendocrinol* 2004; **16**: 308–312.
22 Sabatier N, Leng G. Presynaptic actions of endocannabinoids mediate alpha-MSH-induced inhibition of oxytocin cells. *Am J Physiol Regul Integr Comp Physiol* 2006; **290**: R577–R584.
23 Ciosek J, Cisowska A. Centrally administered galanin modifies vasopressin and oxytocin release from the hypothalamo-neurohypophysial system of euhydrated and dehydrated rats. *J Physiol Pharmacol* 2003; **54**: 625–641.
24 Beene DL, Scott JD. A-kinase anchoring proteins take shape. *Curr Opin Cell Biol* 2007; **19**: 192–198.
25 Coghlan VM, Perrino BA, Howard M, Langeberg LK, Hicks JB, Gallatin WM, Scott JD. Association of protein kinase A and protein phosphatase 2B with a common anchoring protein. *Science* 1995; **267**: 108–111.
26 McConnachie G, Langeberg LK, Scott JD. AKAP signaling complexes: getting to the heart of the matter. *Trends Mol Med* 2006; **12**: 317–323.
27 Pawson T, Nash P. Assembly of cell regulatory systems through protein interaction domains. *Science* 2003; **300**: 445–452.
28 Pawson T, Scott JD. Signaling through scaffold, anchoring, and adaptor proteins. *Science* 1997; **278**: 2075–2080.
29 Colledge M, Dean RA, Scott GK, Langeberg LK, Huganir RL, Scott JD. Targeting of PKA to glutamate receptors through a MAGUK-AKAP complex. *Neuron* 2000; **27**: 107–119.
30 Tavalin SJ, Colledge M, Hell JW, Langeberg LK, Huganir RL, Scott JD. Regulation of GluR1 by the A-kinase anchoring protein 79 (AKAP79) signaling complex shares properties with long-term depression. *J Neurosci* 2002; **22**: 3044–3051.
31 Bal M, Zhang J, Hernandez CC, Zaika O, Shapiro MS. Ca^{2+}/calmodulin disrupts AKAP79/150 interactions with KCNQ (M-Type) K^+ channels. *J Neurosci* 2010; **30**: 2311–2323.
32 Zhang J, Bal M, Bierbower S, Zaika O, Shapiro MS. AKAP79/150 signal complexes in G-protein modulation of neuronal ion channels. *J Neurosci* 2011; **31**: 7199–7211.

33 Carnegie GK, Means CK, Scott JD. A-kinase anchoring proteins: from protein complexes to physiology and disease. *IUBMB Life* 2009; **61**: 394–406.

34 Lester LB, Langeberg LK, Scott JD. Anchoring of protein kinase A facilitates hormone-mediated insulin secretion. *Proc Natl Acad Sci USA* 1997; **94**: 14942–14947.

35 Kashina AS, Semenova IV, Ivanov PA, Potekhina ES, Zaliapin I, Rodionov VI. Protein kinase A, which regulates intracellular transport, forms complexes with molecular motors on organelles. *Curr Biol* 2004; **14**: 1877–1881.

36 Bizzarro V, Petrella A, Parente L. Annexin A1: novel roles in skeletal muscle biology. *J Cell Physiol* 2012; **227**: 3007–3015.

37 Buckingham JC, Solito E, John C, Tierney T, Taylor A, Flower R, Christian H, Morris J. Annexin 1: a paracrine/juxtacrine mediator of glucorticoid action in the neuroendocrine system. *Cell Biochem Funct* 2003; **21**: 217–221.

38 John CD, Christian HC, Morris JF, Flower RJ, Solito E, Buckingham JC. Kinase-dependent regulation of the secretion of thyrotrophin and luteinizing hormone by glucocorticoids and annexin 1 peptides. *J Neuroendocrinol* 2003; **15**: 946–957.

39 Solito E, Mulla A, Morris JF, Christian HC, Flower RJ, Buckingham JC. Dexamethasone induces rapid serine-phosphorylation and membrane translocation of annexin 1 in a human folliculostellate cell line via a novel nongenomic mechanism involving the glucocorticoid receptor, protein kinase C, phosphatidylinositol 3-kinase, and mitogen-activated protein kinase. *Endocrinology* 2003; **144**: 1164–1174.

40 Taylor AD, Cowell AM, Flower J, Buckingham JC. Lipocortin 1 mediates an early inhibitory action of glucocorticoids on the secretion of ACTH by the rat anterior pituitary gland in vitro. *Neuroendocrinology* 1993; **58**: 430–439.

41 Chapman LP, Epton MJ, Buckingham JC, Morris JF, Christian HC. Evidence for a role of the adenosine 5′-triphosphate-binding cassette transporter A1 in the externalization of annexin I from pituitary folliculo-stellate cells. *Endocrinology* 2003; **144**: 1062–1073.

42 Ohnishi M, Tokuda M, Masaki T, Fujimura T, Tai Y, Itano T, Matsui H, Ishida T, Konishi R, Takahara J. Involvement of annexin-I in glucose-induced insulin secretion in rat pancreatic islets. *Endocrinology* 1995; **136**: 2421–2426.

43 Tcatchoff L, Andersson S, Utskarpen A, Klokk TI, Skanland SS, Pust S, Gerke V, Sandvig K. Annexin A1 and A2: roles in retrograde trafficking of Shiga toxin. *PLoS ONE* 2012; **7**: e40429.

44 McArthur S, Yazid S, Christian H, Sirha R, Flower R, Buckingham J, Solito E. Annexin A1 regulates hormone exocytosis through a mechanism involving actin reorganization. *FASEB J* 2009; **23**: 4000–4010.

45 Park JJ, Gondre-Lewis MC, Eiden LE, Loh YP. A distinct trans-Golgi network subcompartment for sorting of synaptic and granule proteins in neurons and neuroendocrine cells. *J Cell Sci* 2011; **124**: 735–744.

46 Fiorini A, Sultana R, Barone E, Cenini G, Perluigi M, Mancuso C, Cai J, Klein JB, St Clair D, Butterfield DA. Lack of p53 affects the expression of several brain mitochondrial proteins: insights from proteomics into important pathways regulated by p53. *PLoS ONE* 2012; **7**: e49846.

47 Cai Q, Lu L, Tian JH, Zhu YB, Qiao H, Sheng ZH. Snapin-regulated late endosomal transport is critical for efficient autophagy-lysosomal function in neurons. *Neuron* 2010; **68**: 73–86.

48 Gondre-Lewis MC, Park JJ, Loh YP. Cellular mechanisms for the biogenesis and transport of synaptic and dense-core vesicles. *Int Rev Cell Mol Biol* 2012; **299**: 27–115.

49 Park JJ, Cawley NX, Loh YP. Carboxypeptidase E cytoplasmic tail-driven vesicle transport is key for activity-dependent secretion of peptide hormones. *Mol Endocrinol* 2008; **22**: 989–1005.

50 Cawley NX, Wetsel WC, Murthy SR, Park JJ, Pacak K, Loh YP. New roles of carboxypeptidase E in endocrine and neural function and cancer. *Endocr Rev* 2012; **33**: 216–253.

51 Moldin SO, Rubenstein JL. *Understanding Autism: From Basic Neuroscience to Treatment*. Boca Raton, FL, CRC Press, 2006.

52 Jacob TC, Kaplan JM. The EGL-21 carboxypeptidase E facilitates acetylcholine release at *Caenorhabditis elegans* neuromuscular junctions. *J Neurosci* 2003; **23**: 2122–2130.

53 Park JJ, Cawley NX, Loh YP. A bi-directional carboxypeptidase E-driven transport mechanism controls BDNF vesicle homeostasis in hippocampal neurons. *Mol Cell Neurosci* 2008; **39**: 63–73.

54 Gauthier LR, Charrin BC, Borrell-Pages M, Dompierre JP, Rangone H, Cordelieres FP, De Mey J, MacDonald ME, Lessmann V, Humbert S, Saudou F. Huntingtin controls neurotrophic support and survival of neurons by enhancing BDNF vesicular transport along microtubules. *Cell* 2004; **118**: 127–138.

55 Kwinter DM, Lo K, Mafi P, Silverman MA. Dynactin regulates bidirectional transport of dense-core vesicles in the axon and dendrites of cultured hippocampal neurons. *Neuroscience* 2009; **162**: 1001–1010.

56 Schlager MA, Kapitein LC, Grigoriev I, Burzynski GM, Wulf PS, Keijzer N, de Graaff E, Fukuda M, Shepherd IT, Akhmanova A, Hoogenraad CC. Pericentrosomal targeting of Rab6 secretory vesicles by bicaudal-D-related protein 1 (BICDR-1) regulates neuritogenesis. *EMBO J* 2010; **29**: 1637–1651.

57 Hendricks AG, Holzbaur EL, Goldman YE. Force measurements on cargoes in living cells reveal collective dynamics of microtubule motors. *Proc Natl Acad Sci USA* 2012; **109**: 18447–18452.

58 Hendricks AG, Perlson E, Ross JL, Schroeder HW 3rd, Tokito M, Holzbaur EL. Motor coordination via a tug-of-war mechanism drives bidirectional vesicle transport. *Curr Biol* 2010; **20**: 697–702.

59 Soppina V, Rai AK, Ramaiya AJ, Barak P, Mallik R. Tug-of-war between dissimilar teams of microtubule motors regulates transport and fission of endosomes. *Proc Natl Acad Sci USA* 2009; **106**: 19381–19386.

60 Traverso V, Morris JF, Flower RJ, Buckingham J. Lipocortin 1 (annexin 1) in patches associated with the membrane of a lung adenocarcinoma cell line and in the cell cytoplasm. *J Cell Sci* 1998; **111**: 1405–1418.

61 Solito E, McArthur S, Christian H, Gavins F, Buckingham JC, Gillies GE. Annexin A1 in the brain–undiscovered roles? *Trends Pharmacol Sci* 2008; **29**: 135–142.